

1 To: Applied and Environmental Microbiology

2

3 **Genomic and phylogenetic analysis of the first myovirus isolated from**  
4 ***Oceanospirillaceae*, representing a novel viral cluster prevalent in**  
5 **polar oceans**

6 **Wenjing Zhang<sup>a†</sup>, Yundan Liu<sup>a†</sup>, Jinyan Xing<sup>b†</sup>, Kaiyang Zheng<sup>a</sup>, Qian Li<sup>c</sup>, Chengxiang Gu<sup>a</sup>,**  
7 **Ziyue Wang<sup>a</sup>, Hongbing Shao<sup>a,d</sup>, Cui Guo<sup>a,d</sup>, Hui He<sup>a,d</sup>, Hualong Wang<sup>a,d</sup>, Yeong Yik Sung<sup>d,e</sup>,**  
8 **Wen Jye Mok<sup>d,e</sup>, Li Lian Wong<sup>d,e</sup>, Yantao Liang<sup>a,d#</sup>, Andrew McMinn<sup>a,f</sup>, Min Wang<sup>a,b,d#</sup>**

9 <sup>a</sup> College of Marine Life Sciences, Frontiers Science Center for Deep Ocean Multispheres and  
10 Earth System, Institute of Evolution and Marine Biodiversity, Ocean University of China, Qingdao  
11 266003, China.

12 <sup>b</sup> The Affiliated Hospital of Qingdao University, Qingdao 266000, China

13 <sup>c</sup> School of Oceanography, Shanghai Jiao Tong University, Shanghai, 200030, China

14 <sup>d</sup> UMT-OUC Joint Centre for Marine Studies, Qingdao 266003, China.

15 <sup>e</sup> Institute of Marine Biotechnology, Universiti Malaysia Terengganu (UMT), 21030, Kuala Nerus,  
16 Malaysia.

17 <sup>f</sup> Institute for Marine and Antarctic Studies, University of Tasmania, Hobart, Tasmania 7001,  
18 Australia.

19

20 Running title: First myovirus infecting *Oceanospirillaceae*

21

22 †These authors contributed equally to this work

23 # Correspondence: [liangyantao@ouc.edu.cn](mailto:liangyantao@ouc.edu.cn) (Y.L.); [mingwang@ouc.edu.cn](mailto:mingwang@ouc.edu.cn) (M.W.)

24

25 **Abstract:** The marine bacterial family *Oceanospirillaceae*, which is abundant in the  
26 deep-seas and polar oceans, is closely associated with algal blooms and petroleum  
27 hydrocarbons degradation. However, only a few *Oceanospirillaceae*-infecting phages  
28 have so far been reported. Here we report on a novel *Oceanospirillum* phage,  
29 vB\_OsaM\_PD0307, which is the first myovirus to be found that infects  
30 *Oceanospirillaceae*. vB\_OsaM\_PD0307 with a 44,421 bp linear dsDNA genome.  
31 Phylogenetic analysis and average nucleotide sequence identities suggest that  
32 vB\_OsaM\_PD0307 is different from other phage isolates and represents a novel genus-  
33 level myoviral cluster with two high-quality uncultured viral genomes, designed as  
34 *Oceanospimyovirus*. Additionally, the biogeographical distribution of the  
35 vB\_OsaM\_PD0307 cluster suggests that they are widespread in the oceans and  
36 abundant in polar areas. In summary, our findings expand the current understanding of  
37 the phylogenetic diversity, genomic characteristic and function of *Oceanospimyovirus*  
38 phages, and highlight the role of the vB\_OsaM\_PD0307 phage as a major ecological  
39 agent that can infect certain key bacterial groups associated with polar algal blooms.

40 **Importance:** *Oceanospirillum* phage vB\_OsaM\_PD0307 is the first myovirus found to  
41 infect *Oceanospirillaceae* and represents a novel viral genus, *Oceanospimyovirus*. This  
42 study provides insights into the genomic, phylogenetic, and ecological characteristics  
43 of myoviruses infecting *Oceanospirillaceae* and improves our understanding of the  
44 interactions between *Oceanospirillaceae* and their phages in the oceans.

45 **Keywords:** *Oceanospirillum* phage vB\_OsaM\_PD0307, *Oceanospimyovirus*, Genomic

46 and phylogenetic analysis, Ecological distribution

47

## 48 **Introduction**

49 Viruses are the most abundant and diverse “life forms” in the ocean (1, 2). They mediate  
50 fluctuations in microbial abundance and shape community structure and aggregation  
51 through the lysis of their hosts, processes referred to as the “viral shunt” and “viral  
52 shuttle” (3–5). Heterotrophic bacteria-infecting phage in particular, can cause over 50%  
53 mortality rate of their hosts through cell lysis, and this number can be higher in certain  
54 environments (6). Viral-host interactions promote marine biogeochemical cycles and  
55 marine carbon sequestration through the processes known as the “biological pump”  
56 and “microbial carbon pump”. Phages also promote the active evolution and shape  
57 phylogeny of their hosts through horizontal gene transfer (7, 8). Over the past few  
58 decades, our understanding of viral diversity has significantly expanded, though mostly  
59 relying on the development of high-throughput sequencing and metagenomic  
60 technology. As a consequence, over 90% of available viral genomes remain uncultured  
61 and uncharacterized (there in after referred to as UViGs) (9). Targeted phage isolation  
62 methods are vital in terms of filling the knowledge gaps between sequences information  
63 and functionality, especially in the context of interaction dynamics and co-evolution  
64 between phage and host, as well as shedding light on their potential role in marine  
65 microbial food webs. .

66 The bacteria genus *Oceanospirillum*, Hylemon was separated from the genus



67 *Spirillum* based on their differing physiological properties and DNA base composition.

68 The mean GC content of *Oceanospirillum* genomes ranges from 42 to 51 mol% (10,

69 11). Currently, twenty-three members have been validly published

70 (<https://www.bacterio.net/genus/Oceanospirillum>) and these have been isolated from a

71 range of marine environments, including coastal waters (10, 12), decaying seaweed (13),

72 mangrove sediments (14, 15), putrid infusions of marine mussels (11, 16, 17) and the

73 leaves of the seagrass (18). Bacteria within this family are well known for their

74 capability of hydrocarbon degradation (19–22) and so are often detected at high

75 abundances in oil-contaminated marine environments (23–25). Recently, a high

76 abundance of *Oceanospirillaceae* was detected in the hadal zone of the Mariana Trench

77 (21), suggesting their potential importance in these extreme marine habitats. In addition,

78 *Oceanospirillaceae* are also prevalent in polar oceans, such as the Amundsen Sea

79 polynya (26, 27), Ross Sea (28) and coastal waters of the Arctic (29). Members of

80 *Oceanospirillaceae* possess a complete B12 vitamin synthesis pathway, which affects

81 DMSP synthesis and promotes algal growth (30), suggesting that *Oceanospirillaceae*

82 plays an important role in some algal blooms. Despite the ecological significance of

83 *Oceanospirillaceae* in the ocean, our understanding of their co-occurring phages is still

84 poor. Currently, only eight phages infecting *Oceanospirillaceae* have been isolated,

85 including three autographiviruses infecting *Marinomonas*, two siphoviruses, and one

86 corticovirus, and two unclassified phages (*Marinomonas* phage MfV and *Nitrincola*

87 phage 1M3-16). There have been no previous reports of Myovirus infecting

88 *Oceanospirillaceae*.

89 In this study, the first myovirus infecting *Oceanospirillaceae*, named  
90 vB\_OsaM\_PD0307 was isolated and characterized its genomic and phylogenetic  
91 features. Phylogenetic analysis showed that vB\_OsaM\_PD0307 was distantly related  
92 to other reported viral isolates in the NCBI dataset and may represent a novel myoviral  
93 genus with two high-quality UViGs. The biogeographic distribution analysis suggests  
94 that the homologous of vB\_OsaM\_PD0307 are abundant in polar oceans. This study  
95 provides an insight into the genome of *Oceanospirillaceae* myovirus, shedding light on  
96 the important interactions between algal bloom-associated bacteria and myoviruses in  
97 polar oceans.

98

## 99 **Materials and methods**

### 100 **Isolation and purification of host phage strain**

101 Both *Oceanospirillum* sp. PD0307 and its phage vB\_OsaM\_PD0307 were isolated from  
102 a surface water sample collected from coastal waters of the Yellow Sea (120°19'32.6"E,  
103 36°4'1.7"N) in June 2020. The host strain was isolated from and maintained in 2216E  
104 medium (peptone 5 wt.%, yeast extract 1 wt.%), at 28 °C and 120 rpm, in a shaking  
105 incubator.

106 For phage isolation, 10 ml seawater sample collected from the same station was  
107 passed through a 0.22 µm membrane filter to remove any cellular organisms (Isopore™  
108 0.2 µm GTTP; Merck, Ireland) (31). Phage vB\_OsaM\_PD0307 was isolated by plaque

109 assay using the double-layer plating method. Briefly, 200  $\mu$ l seawater filtered 0.22  $\mu$ m  
110 pore-size filters was mixed with the host culture (approximately 8-hour) and incubated  
111 for 30-minute, allowing the absorption of the phages at room temperature. Then, 4 ml  
112 of the semi-solid culture (at 55 °C) was added to the mixture, pouring it onto the plate  
113 after vortexing. Plates were cultivated at 28 °C and monitored until visible plaques were  
114 formed in the double layer culture (usually happens within 24 h).

115 A single plaque was picked from the double plate and suspended in 2 ml of SM  
116 buffer, (100 mM of NaCl, 8 mM of MgSO<sub>4</sub>, 50 mM of Tris-HCl, at pH 7.5) and then  
117 purified three times via plaque assay. Culture lysates were recovered to enrich and  
118 concentrate the phages. Approximately 500 ml of exponentially growing host were  
119 challenged with 50ml purified viral stock and incubated at 28 °C for 24 h. The lysate  
120 was first filtered through a 0.22  $\mu$ m membrane filter to remove uninfected host cells,  
121 then concentrated from 500 ml to 5 ml using 30 kDa super-filters (UFC5030, Millipore).  
122 Concentrated phage lysate was treated with a second filtration by passing through 0.22  
123  $\mu$ m Supor membrane.

#### 124 **Preparation for phage morphology observation**

125 Phage particles were precipitated by adding PEG 8000 and NaCl to a final concentration  
126 of 10% (w/v) and 1 M, respectively, and incubated overnight at 4°C. Phage particles  
127 were precipitated by centrifugation at 15,000 g for 30 min and then re-suspended in 5  
128 ml of SM buffer, 20  $\mu$ l of the mixture was then taken and placed on a copper net and  
129 stained with 2 wt.% phosphotungstic acids (pH 7.5) for 5 min. Its morphology was

130 identified using transmission electron microscope (TEM) (JEOLJEM-1200EX, Japan)  
131 at 100 KV, equipped with a diamond knife for thin sectioning, and Images were taken  
132 using GATAN INC CCD image transmission system (Gatan Inc., Pleasanton, CA,  
133 USA).

#### 134 **Phage DNA preparation, genome sequencing and gene annotation**

135 The concentrated phage lysate was prepared for phage genomic DNA extraction was  
136 performed by Virus DNA Kit (OMEGA), according to the manufacturer's instructions,  
137 and quality control was subsequently carried out on the purified DNA samples. The  
138 high-quality DNA sample (OD<sub>260/280</sub>=1.8~2.0, >6ug) was used to construct the  
139 fragment library and then used for Illumina NovaSeq 6000 sequencing by Shanghai  
140 Biozeron Biotechnology Co., Ltd. (Shanghai, China.). The raw paired-end reads were  
141 trimmed and quality controlled by Trimmomatic (v. 0.3.6) with parameters:  
142 SLIDINGWINDOW:4:15, MINLEN:75 (32). ABySS was used to assemble the viral  
143 genome after the quality control processes, multiple-Kmer parameters were chosen to  
144 obtain the optimal assembly results (33). GapCloser software was subsequently applied  
145 to fill in the remaining local inner gaps and to correct the single base polymorphism for  
146 the final assembly and further analysis (34).

147 Gene models were identified using GeneMarkS (35). Then all gene models were  
148 blastp against non-redundant (NR) in the NCBI database, SwissProt (<http://uniprot.org>),  
149 KEGG (<http://www.genome.jp/kegg/>), and COG (<http://www.ncbi.nlm.nih.gov/COG>)  
150 for functional annotation by the blastp module. The genome visualization was

151 conducted by CLC Main Workbench (v6.8 downloaded on <http://www.clcbio.com>). In  
152 addition, tRNA was identified using the tRNAscan-SE (v1.23) (36) and rRNA was  
153 determined using RNAmmer (v1.2 downloaded on  
154 <https://services.healthtech.dtu.dk/service.php/RNAmmer-1.2>). GC skew analysis was  
155 performed on Genskew (<https://genskew.csb.univie.ac.at/webskew>). Average amino  
156 acid identity (AAI) between vB\_OsaM\_PD0307 and other viral sequences was  
157 calculated by the AAI calculator (<http://enve-omics.ce.gatech.edu>) to estimate the  
158 distribution of AAI between proteins from two genomic sequences.

#### 159 **Phylogenic tree construction of host *Oceanospirillaceae* sp.**

160 A total of 355 16S rRNA sequences of *Oceanospirillaceae* with defined taxonomy in  
161 GenBank, including the host strain *Oceanospirillum* sp. PD0307, were retrieved from  
162 GenBank and aligned by MAFFT (37) using G-INS-1 of strategy with 1000 iterations  
163 (`mafft --globalpair --maxiterate 1000 16S_Oceanospirillaceae_pro.fasta >`  
164 `16S_Oceanospirillaceae.mafft`). The likelihood phylogenic tree was calculated from  
165 multiple sequence alignments using IQ-tree2 (38), applying the GTR+I+G model with  
166 1000 bootstrap iterations (Command: `iqtree -s 16S_Oceanospirillaceae.mafft -m MFP`  
167 `-B 1000 -T AUTO`) and visualized by iTOL v4 (39).

#### 168 **Homologous sequence recruitment of phage vB\_OsaM\_PD0307**

169 A total of 57212 isolated complete phages genomes were downloaded from NCBI  
170 GenBank to build a reference isolated-phages dataset  
171 (<https://www.ncbi.nlm.nih.gov/labs/virus>). The whole genome sequences of phage

172 vB\_OsaM\_PD0307 as a input to find the other similar genomes by blastn in this  
173 reference isolated-phages dataset with e-value  $< 1e-5$ , identity  $> 50\%$ . At the same time,  
174 homology recruitment in uncultured virus databases was also taking place. The whole  
175 genome sequence of phage vB\_OsaM\_PD0307 was queried against the IMG/VR v3  
176 (40) database using blastn to search for homologous contig sequences (threshold: e-  
177 value  $< 1e-5$ , percentage of identity  $> 70\%$ ) and seven UViGs were retrieved.

178 All the isolated and uncultured homologous sequences with vB\_OsaM\_PD0307,  
179 and all eight isolated *Oceanospirillaceae* phages were combined to calculate  
180 intergenomic similarity by VIRIDIC (41), as well as ANI via OAT software using the  
181 orthogonal method to determine the overall similarity (42). AAI was calculated on the  
182 website (<http://enve-omics.ce.gatech.edu>), which estimated the distribution of AAI  
183 between proteins from the two genomic sequences.

#### 184 **Phylogenetic and comparative genomic analysis**

185 A proteomic tree based on the similarities of the whole genome was generated using  
186 VIPTree (43). Each encoding nucleic sequence as a query was searched against the  
187 Virus-Host DB using tBLASTx. All viral sequences in Virus-Host DB were selected to  
188 generate a first circular tree. The second more accurate phylogenetic tree was  
189 regenerated using 35 related phages automatically selected from the first results. 20  
190 isolated sequences were selected as references, and seven *Mycobacterium* phages  
191 appeared as an outgroup, vB\_OsaM\_PD0307 and the other seven UViGs were used as  
192 queries to construct the whole-genome phylogenetic tree using VIPTree (43). The group

193 of seven UViGs, *Shewanella* phage SppYZU01, and vB\_OsaM\_PD0307 were selected  
194 to perform the multi-genomic alignments.

195 **Global oceanic distribution of phage vB\_OsaM\_PD0307 and relative viral**  
196 **sequences**

197 Stations in Global Ocean Viromes 2.0 (GOV 2.0) were divided into five viral ecological  
198 zones (VEZs), including the Arctic (ARC), Antarctic (ANT), temperate and tropical  
199 epipelagic (EPI), temperate and tropical mesopelagic (MES), and bathypelagic  
200 (BATHY). Five representative stations were selected for each VEZs to assess the  
201 relative abundance of vB\_OsaM\_PD0307 and its relative viral sequences. (ANT:  
202 ERR594377, ERR594409, ERR599352, ERR599364, ERR599384; ARC:  
203 ERR2762158, ERR2762161, ERR2762163, ERR2762165, ERR2762169; EPI:  
204 ERR594353, ERR594398, ERR594395, ERR594403, ERR594376; MES:  
205 ERR2752153, ERR2752154, ERR2752163, ERR599375, ERR599379; BATHY:  
206 msp112, msp121, msp131, msp144, msp81) The global oceanic distribution was  
207 calculated by the metagenomics tool minimap2 (parameters: -min-read-percent-identity  
208 0.95, -min-read-aligned-percent 0.75, -m rpkm) (46) and expressed by RPKM (reads  
209 per kilobase per million mapped reads) values. Besides, pelagiphage HTVC010P,  
210 HTVC011P, cyanophages P-SSP7, P-SSM7, S-SM2, S-CBS2, roseophage SIO1,  
211 SAR116 phage HMO2011 which have significantly representative in different oceanic  
212 areas and depths as the references.

213 **Data availability**

214 The complete genome of *Oceanospirillum* phage vB\_OsaM\_PD0307 has been  
215 deposited in NCBI GeneBank under accession number OL658619, and the 16S rRNA  
216 sequence of the host also has been deposited in NCBI GeneBank under accession  
217 number OL636378.

218

## 219 **Results and Discussion**

### 220 **Isolation and morphology of the plaques of vB\_OsaM\_PD0307**

221 The phage vB\_OsaM\_PD0307 (accession: OL658619), infecting *Oceanospirillum* sp.  
222 PD0307 (accession: OL636378), was isolated from a surface seawater sample from the  
223 Yellow Sea. The morphology of vB\_OsaM\_PD0307 was that of a myovirus with an  
224 icosahedral head of  $51 \pm 2$  nm in length and a  $112 \pm 3$  nm-long contractile tail (Fig. 1A).  
225 Infection of vB\_OsaM\_PD0307 formed clear and round (1–2 mm diameter average)  
226 plaques in double-layer culture (Fig. 1B).

### 227 **Phylogenetic analysis of the host bacterium *Oceanospirillum* sp. PD0307**

228 The phylogenic position of the host bacterium *Oceanospirillum* sp. PD0307 was  
229 clustered with other *Oceanospirillaceae* strains in the phylogenetic tree. The  
230 monophyletic clade containing *Oceanospirillum* sp. PD0307 includes four genera  
231 (*Neptuniibacter*, *Profundimonas*, *Amphritea*, and *Oceanospirillum*), indicating its close  
232 relationship with other *Oceanospirillaceae*, especially with other *Oceanospirillum*  
233 strains (Fig. 2). Although *Oceanospirillum* sp. PD0307 is on a sister branch with  
234 *Oceanospirillum sanctuarii* AK56, which was isolated from sediment (14), the branch



235 with *Oceanospirillum* sp. PD0307 has a relatively distant phylogenetic link with them,  
236 suggesting *Oceanospirillum* sp. PD0307 might be a novel species of *Oceanospirillum*.  
237 In addition, *Oceanospirillum* sp. PD0307 has the longest branch length in the tree  
238 (0.121), indicating that *Oceanospirillum* sp. PD0307 might have evolved from a  
239 common ancestor of *Oceanospirillum* or even *Oceanospirillaceae*. Thus, the interaction  
240 between phage vB\_OsaM\_PD0307 and *Oceanospirillum* sp. PD0307 might represent  
241 a novel case in the co-evolutionary history between viruses and *Oceanospirillum*.

#### 242 **Genomic features of phage vB\_OsaM\_PD0307**

243 According to the genomic sequencing and assembly results, phage vB\_OsaM\_PD0307  
244 has a 44,421-bp linear dsDNA genome with a GC content of 57.13%. No tRNA and  
245 rRNA genes were found in the genome. The genome had a 96.41% encoding rate  
246 consisting of 56 predicted open reading frames (ORFs). Thirty-seven ORFs are located  
247 on the sense strand, accounting for 66.07% of the total coding genes, and nineteen ORFs  
248 on the antisense strand (Fig. 3A, Table S1). There were 11 coding regions (19.64 %  
249 ORF angles) that did not match any homologous sequence under the restriction of *e*-  
250 value < 1e-5 in all 56 genes. Among the remaining 45 genes that matched homologous  
251 sequences, 23 identified specific functions, and 22 matched homologous proteins  
252 containing unknown functions. The 23 functional ORFs could be classified into three  
253 different modules: twelve ORFs for DNA replication and metabolism, ten ORFs for  
254 phage structure and packing proteins, and one auxiliary metabolic gene (AMG,  
255 transcriptional regulator) (Fig. 3A).

256 In the genome of phage vB\_OsaM\_PD0307, twelve ORFs were predicted to encode  
257 genes related to DNA replication and metabolism. ORF 25 encoded the D-Ala-D-Ala  
258 carboxypeptidase family metallohydrolase gene, and also showed high homology with  
259 hedgehog signaling/DD-peptidase zinc-binding domain gene of *Vibrio* phage  
260 1.169.O\_10N.261.52.B (pident 58.6, qcovhsp 100, bitscore 154.1, evalue 4.4E-34).  
261 The structure of the N-terminal signaling domain of hedgehog proteins has been  
262 resolved and reveals a tetrahedrally coordinated zinc ion, which is structurally  
263 homologous to the zinc-binding motif in bacterial D-alanyl-D-alanine  
264 carboxypeptidases (DD-peptidases) (44–46). ORF 25 contained some amino acids of  
265 peptidase genes, commonly detected within some bacterial genomes, such as motifs  
266 HXXXXXXD and WXH, which were typical motifs for peptidase M15 subfamily A  
267 (47, 48). ORFs 44 and 45 encoded DNA-methyltransferase and DNA methylase genes,  
268 respectively. Site-specific DNA-methyltransferase, N-6 adenine-specific DNA  
269 methylase, and cytosine-N4-specific are enzymes that specifically methylate the amino  
270 group at the C-4 position of cytosines and the N-6 position of adenine in DNA. They  
271 utilize the cofactor S-adenosyl-L-methionine as the methyl donor and are active as  
272 monomeric enzymes. In prokaryotes, the major role of DNA methylation is to protect  
273 host DNA against degradation by restriction enzymes (49, 50), and DNA methylation  
274 of phage vB\_OsaM\_PD0307 may have a similar function to elude host immunity.

275 Ten ORFs encoding genes related to the structure and packaging modules are  
276 located at the front end of the genome. The putative protease gene (ORF 7) is affiliated

277 with the cl23717 superfamily, which has portal proteins upstream and capsid proteins  
278 downstream. Capsid maturation in double-stranded-DNA (dsDNA) phages requires  
279 proteolytic cleavage by a prohead protease (51). In the BLAST results, ClpP/crotonase-  
280 like domain proteins were significantly matched to the S49 family proteins, members  
281 of the large crotonase superfamily (52). One of the typical features of myotail phages  
282 is the presence of tail sheath proteins. ORF 13 encoded these in Phage  
283 vB\_OsaM\_PD0307, which had a strong homologous sequence with the myophage  
284 *Shewanella* phage SppYZU01 with 99% qcov and 66.87% pident. The top 50  
285 homologous sequences are all present in the myophages under the given thresholds (*e*-  
286 value < 1e-50, qcov > 90%, pident > 30%). The TMhelix (ORF 17) containing gene,  
287 which is sandwiched between two tail genes, is related to the transport of substances  
288 across cell membranes (53) and may be related to the adsorption of host bacteria by  
289 phages.

290 Only one AMG was detected in the genome of phage vB\_OsaM\_PD0307 and this  
291 encoded a gene related to the TetR family transcriptional regulator (ORF 46). It is well  
292 represented and widely distributed among bacteria with an HTH DNA-binding motif  
293 (54). Members of this family are well known for their roles as regulators of antibiotic  
294 efflux pumps. This gene is a phage-mediated transcriptional regulator for antimicrobial  
295 resistance and can help host cells to survive in antimicrobial environments (55).

296 Cumulative GC skew analyses were performed to determine the origin and  
297 terminus of replication of the phage genome (56). The minimum GC skew was at 300

298 nt and the maximum at 43900 nt, which are at the head and tail of the genome  
299 respectively (Fig. 3B). Two inflection points were identified in the above regions,  
300 indicating an asymmetric base composition, which were lowest at the origin and the  
301 highest at the terminus.

302 **Phylogenetic and synteny analysis between phage vB\_OsaM\_PD0307 and its**  
303 **homologous sequences**

304 To further understand the phylogenetic relationship between phage vB\_OsaM\_PD0307  
305 and other isolated phages, 1,812 dsDNA phage genomes were selected from the Virus-  
306 Host database to establish the whole-genome phylogenetic tree. Of these, phage  
307 vB\_OsaM\_PD0307 originated from the tree root and formed a separate clade (Fig. 4A).  
308 The detailed phylogenetic trees were then regenerated after adding the seven  
309 homologous UViGs. Phage vB\_OsaM\_PD0307, *Shewanella* phage SppYZU01, and  
310 the seven homologous UViGs were grouped together and formed a unique viral cluster  
311 (Figs. 4B and 4C). Among them, S85\_DCM\_NO\_526, S137 and UViG\_281 were very  
312 close to vB\_OsaM\_PD0307 and shared the same ancestral branch, indicating that they  
313 had the same evolutionary characteristics and similar genetic relationships.

314 To clarify the common features of phage vB\_OsaM\_PD0307 and homologous  
315 viral genomes, an alignment of these sequences by tBLASTx was performed.  
316 Comparative genomic analysis revealed that they had a universal homology at the  
317 amino acid level, especially among vB\_OsaM\_PD0307, S85\_DNC\_NO\_526 and  
318 S137\_MES\_NO\_1159 (Fig. 4D). These three viral genomes showed a high degree of

319 synteny in the whole-genome arrangement, indicating correlations in the phylogenetic  
320 process. Most structural and packaging gene similarities suggest that these viruses may  
321 be taxonomically similar. Given that this is the first isolate of this group of viruses, it is  
322 likely that this is a new and undiscovered group of viruses. Even the only AMG of  
323 vB\_OsaM\_PD0307, the TetR family transcriptional regulator gene, can be found in a  
324 similar region to the other two homologous viral genomes. This suggests that this viral  
325 group may possess the ability to assist host cells survive environmental antibiotics. It is  
326 worth noting that genes A, B and C of vB\_OsaM\_PD0307, which encode the portal  
327 protein, TMhelix containing protein and hypothetical protein respectively, were  
328 common but not homologous among the group; this may relate to the range of hosts of  
329 these viruses.

### 330 **vB\_OsaM\_PD0307 represented a new myoviral genus**

331 Based on the results of homology search in the reference isolated-phages dataset, only  
332 one genome, Shewanella phage SppYZU01, was retrieved, with a relatively low  
333 average amino acid identity (AAI, 48.33%) and average nucleotide sequence identity  
334 (ANI, 62.16%). Therefore, BLASTn was used to search the IMG/VR v3 (40) database  
335 to find the homologous UViG sequences. In total seven UViGs, under the thresholds  
336 (min pident 70.21%, and min e-value 1.60E-08), were screened. They were all  
337 assembled from marine waters or sediment samples, three of them were judged as high-  
338 quality sequences (i.e. genome  $\geq$ 90% complete and non-redundant) and four contigs  
339 were judged as genome fragments (i.e. genome <90% complete). The longest and

340 shortest sequences were 43.16 and 8.41 kb, respectively (Table S2).

341 All eight complete genomes of the isolated *Oceanospirillaceae*-infecting phages  
342 and the eight homologous sequences with vB\_OsaM\_PD0307 were combined and the  
343 intergenomic similarity of the seventeen sequences were analysed using VIRIDIC (41).  
344 Three *Marinomonas* phages assigned to the same genus, *Murciavirus* shared high  
345 intergenomic similarity (> 95%), and their aligned genome fraction and genome lengths  
346 were all 100%. In addition, the viral genomes infecting *Oceanospirillaceae* are diverse  
347 and almost all were quite different from each other (Fig. 5). Of the eight  
348 vB\_OsaM\_PD0307 related homologous UViGs, three sequences in the red box of the  
349 heatmap shared a high intergenomic similarity (> 50%) and had a similar aligned  
350 genome fractions and genome lengths (Fig. 5A). IMGVR\_UViG\_281 and  
351 vB\_OsaM\_PD0307 had a higher aligned genome fraction (80%), but their intergenomic  
352 similarity was low because of the differences in their genome length. The genome  
353 length of IMGVR\_UViG\_281 was only 8,415bp (Table S2).

354 To further define the similarity between vB\_OsaM\_PD0307 and its homologous  
355 sequence, the ANI and AAI of all eight homologous sequences were calculated and the  
356 results were found to be consistent with VIRIDIC. S85\_DCM\_NO\_526,  
357 S137\_MES\_NO\_1159 and IMGVR\_UViG\_281 were similar to vB\_OsaM\_PD0307  
358 with high ANI and AAI values (> 70%) (Fig. 6, Table 1, Fig. S1, Table S3). The  
359 Bacterial and Archaeal Viruses Subcommittee (BAVS) of the International Committee  
360 on the Taxonomy of Viruses (ICTV) considers phages sharing  $\geq 70\%$  ANI as members

361 of the same genus (57). As vB\_OsaM\_PD0307 is the first isolated myovirus infecting  
362 *Oceanospirillaceae* and as it is distant from other isolated phages, based on the  
363 phylogenetic and synteny analysis, it is suggested that vB\_OsaM\_PD0307 represents a  
364 novel viral genus within the Myoviridae, named *Oceanospimyovirus*.  
365 S85\_DCM\_NO\_526 and S137\_MES\_NO\_1159 belong to this new genus together with  
366 vB\_OsaM\_PD0307. IMGVR\_UViG\_281 might also belong to the genus  
367 *Oceanospimyovirus* but having a low-quality genome sequence (Fig. 5B).

#### 368 **Distribution of vB\_OsaM\_PD0307 in the global ocean viromes**

369 The biogeographical distribution of vB\_OsaM\_PD0307 and its closely associated viral  
370 sequences was characterized in the Global Ocean Viromes (GOV2.0) data set covering  
371 five viral ecological zones (VEZs). The reference genomes include *Shewanella* phage  
372 SppYZU01, seven homologous UViGs, and eight typical phages infecting the most  
373 abundant bacterial genera, such as *Pelagibacter*, *Prochlorococcus*, *Synechococcus*,  
374 *Roseobacter* and S116 cluster. The relative abundances confirmed the high abundances  
375 of pelagiphages and cyanophages, as shown in previous studies from Pacific, Indian,  
376 and Global Ocean viromes (58–60). vB\_OsaM\_PD0307 and its associated viral  
377 sequences have a wide and diverse distribution.

378 vB\_OsaM\_PD0307 and S137\_MES\_NO\_1159 have similar distribution patterns,  
379 mostly in MES. Interestingly, S85\_DCM\_NO\_526 and S82\_SUR\_NO\_687 were  
380 relatively abundant in the ANT, while S201\_DCM\_NO\_1678 was relatively abundant  
381 in the ARC (Fig. 6), which was significantly different from the distribution pattern of

382 vB\_OsaM\_PD0307. As viral abundance was mostly tightly coupled to that of their host  
383 cells, it is proposed that annual marine polar algal blooms might be responsible for the  
384 high abundance of *Oceanospirillaceae* (61) and thus the high abundance of  
385 *Oceanospimyovirus* in polar oceans (Fig. 7). In coastal waters of the western Antarctic  
386 Peninsula, *Oceanospirillales* and *Pelagibacteraceae* were most abundant in winter and  
387 spring. In the Amundsen Sea polynya, *Oceanospirillaceae* is one of the principal  
388 dominating bacteria families and in bloom events can contribute up to a 33.9% of the  
389 total bacterial 16S rRNA genes (26, 62–64). In the Meade River area of the coastal  
390 Arctic, OTUs related to the family *Oceanospirillaceae* comprised the largest  
391 component of *Gammaproteobacteria*, approximately 22 and 8% of the bacterial  
392 communities in April and August, respectively (29). Although the reasons for the high  
393 abundance of host cells in the Arctic and Antarctic are not completely understood, it is  
394 hypothesized that: annual algal blooms in polar regions could release large amounts of  
395 organic matter that promotes increased bacterial biodiversity (65–67). In addition, algae  
396 acquire vitamin B12 through a symbiotic relationship with bacteria (68). Members of  
397 *Oceanospirillaceae* have been shown to support phytoplankton growth in polar waters  
398 through the synthesis of cobalamin (vitamin B12) (69–72).

399 Therefore, uncultured viral sequences assembled from the polar viromes might  
400 play an important but unrecognized role in regulating the polar bacterial community  
401 structure associated with polar algal blooms. This study reinforces the importance and  
402 power of the combination of phage isolation and metagenomics to improve our



403 knowledge of marine viral diversity and their ecological significance.

404

## 405 **Conclusion**

406 *Oceanospirillum* has a strong metabolic capacity and a key ecological niche; as such its

407 phage will inevitably affect its abundance, community structure, and metabolic capacity.

408 Here we isolated the first myovirus infecting *Oceanospirillaceae*, named

409 vB\_OsaM\_PD0307. The presence of TetR family transcriptional regulator encoded by

410 vB\_OsaM\_PD0307 suggests its potential contribution to the antimicrobial resistance

411 and virulence of its host. vB\_OsaM\_PD0307 represents a novel myoviral genus-level

412 cluster, named *Oceanospimyovirus*, with two high-quality UViGs. The relative

413 abundance and distribution of *Oceanospimyovirus* suggest that it could be prevalent in

414 polar oceans, coupling with their high-abundant and algal-associated host bacterial

415 communities. The discovery of *Oceanospimyovirus* in the Global Ocean Viromes raised

416 several questions regarding their diversity, ecology, and roles in microbial communities.

417 Here, we performed a culture-based and metagenomics-based analysis of the genomic

418 diversity and distribution of the *Oceanospimyovirus* group. The obtained

419 *Oceanospimyovirus* type genome vB\_OsaM\_PD0307 helps reveal the genuine extent

420 of the genetic diversity of *Oceanospimyovirus* within natural populations of marine

421 viruses. These novel insights into the diversity and ecology of *Oceanospimyovirus*

422 further expands our current understanding of these important phages. Lastly, further

423 investigation using our newly constructed virus–host models will provide additional

424 valuable insights into the influence of viruses on the interaction among algal blooms,  
425 bacteria and viruses in the polar oceans.

426

#### 427 **Acknowledgments**

428 We sincerely thank Jia Zhen, School of Computer Science and Technology, Guizhou  
429 University, for his help in the data processing. We thank for the support of the high-  
430 performance servers of Center for High Performance Computing and System  
431 Simulation, Pilot National Laboratory for Marine Science and Technology (Qingdao),  
432 the Marine Big Data Center of Institute for Advanced Ocean Study of Ocean University  
433 of China, the IEMB-1, a high-performance computing cluster operated by the Institute  
434 of Evolution and Marine Biodiversity, and the high-performance servers of Frontiers  
435 Science Center for Deep Ocean Multispheres and Earth System.

436

#### 437 **Funding information**

438 This study was supported by these fundings: National Natural Science Foundation of  
439 China (No. 41976117, 42120104006, and 42176111), and the Fundamental Research  
440 Funds for the Central Universities (202072002, 201812002, Andrew McMinn).

441

#### 442 **Conflict of interest**

443 The authors declare that they have no conflict of interest regarding this study.

444

445 **Ethical Approval**

446 This article does not contain any studies with animals or human participants performed  
447 by any of the authors.

448

449 **REFERENCES**

- 450 1. Suttle CA. 2005. Viruses in the sea. *Nature* 437:356–361.
- 451 2. Wommack KE, Colwell RR. 2000. Virioplankton: Viruses in Aquatic  
452 Ecosystems. *Microbiol Mol Biol Rev* 64:69–114.
- 453 3. Poulton. AJ. 2021. Shunt or shuttle. *Nat Geosci* 14:180–181.
- 454 4. Suttle CA. 2007. Marine viruses - Major players in the global ecosystem. *Nat*  
455 *Rev Microbiol* 5:801–812.
- 456 5. Brum JR, Sullivan MB. 2015. Rising to the challenge: Accelerated pace of  
457 discovery transforms marine virology. *Nat Rev Microbiol* 13:147–159.
- 458 6. Fuhrman JA. 1999. Marine viruses and their biogeochemical and ecological  
459 effects. *Nature* 399:541–548.
- 460 7. Pál C, Papp B, Lercher MJ. 2005. Adaptive evolution of bacterial metabolic  
461 networks by horizontal gene transfer. *Nat Genet* 37:1372–1375.
- 462 8. Moreau H, Piganeau G, Desdevises Y, Cooke R, Derelle E, Grimsley N. 2010.  
463 Marine Prasinovirus Genomes Show Low Evolutionary Divergence and  
464 Acquisition of Protein Metabolism Genes by Horizontal Gene Transfer. *J Virol*  
465 84:12555–12563.

- 466 9. Gregory AC, Zayed AA, Conceição-Neto N, Temperton B, Bolduc B, Alberti  
467 A, Ardyna M, Arkhipova K, Carmichael M, Cruaud C, Dimier C, Domínguez-  
468 Huerta G, Ferland J, Kandels S, Liu Y, Marec C, Pesant S, Picheral M, Pisarev  
469 S, Poulain J, Tremblay JÉ, Vik D, Acinas SG, Babin M, Bork P, Boss E,  
470 Bowler C, Cochrane G, de Vargas C, Follows M, Gorsky G, Grimsley N, Guidi  
471 L, Hingamp P, Iudicone D, Jaillon O, Kandels-Lewis S, Karp-Boss L, Karsenti  
472 E, Not F, Ogata H, Poulton N, Raes J, Sardet C, Speich S, Stemmann L,  
473 Sullivan MB, Sunagawa S, Wincker P, Culley AI, Dutilh BE, Roux S. 2019.  
474 Marine DNA Viral Macro- and Microdiversity from Pole to Pole. *Cell*  
475 177:1109–1123.
- 476 10. Hylemon PB. 1971. A taxonomic study of the genus *Spirillum* ehrenberg, with  
477 special reference to nutrition and carbohydrate catabolism.
- 478 11. Pot B, Gillis M, Hoste B, Van De Velde A, Bekaert F, Kersters K, De Ley J.  
479 1989. Intra- and intergeneric relationships of the genus *Oceanospirillum*. *Int J*  
480 *Syst Bacteriol* 39:23–24.
- 481 12. Trachtenberg AM, Carney JG, Linnane JD, Rheaume BA, Pitts NL, Mykles  
482 DL, MacLea KS. 2017. Draft genome sequence of the salt water bacterium  
483 *Oceanospirillum linum* ATCC 11336T. *Genome Announc* 5:49–50.
- 484 13. Krieg NR. 1981. The Genera *Spirillum*, *Aquaspirillum*, and *Oceanospirillum*.  
485 *The Prokaryotes* 595–608.
- 486 14. Sidhu C, Thakur S, Sharma G, Tanuku NRS, Pinnaka AK. 2017.

- 487            *Oceanospirillum sanctuarii* sp. Nov., Isolated from a sediment sample. *Int J*  
488            *Syst Evol Microbiol* 67:3428–3434.
- 489    15.    Krishna KK, Bhumika V, Thomas M, Anil Kumar P, Srinivas TNR. 2013.  
490            *Oceanospirillum nioense* sp. nov., a marine bacterium isolated from sediment  
491            sample of Palk bay, India. *Antonie van Leeuwenhoek, Int J Gen Mol Microbiol*  
492            103:1015–1021.
- 493    16.    Terasaki Y. 1979. Transfer of five species and two subspecies of *Spirillum* to  
494            other genera (*Aquaspirillum* and *Oceanospirillum*), with emended descriptions  
495            of the species and subspecies. *Int J Syst Bacteriol* 29:130–44.
- 496    17.    Rosenberg E, DeLong EF, Lory S, Stackebrandt E, Thompson F. 2013. The  
497            prokaryotes: Gammaproteobacteria *The Prokaryotes: Gammaproteobacteria*.
- 498    18.    Weidner S, Arnold W, Stackebrandt E, Pühler A. 2000. Phylogenetic analysis  
499            of bacterial communities associated with leaves of the seagrass *Halophila*  
500            stipulacea by a culture-independent small-subunit rRNA gene approach.  
501            *Microb Ecol* 39:22–31.
- 502    19.    Kleindienst S, Paul JH, Joye SB. 2015. Using dispersants after oil spills:  
503            Impacts on the composition and activity of microbial communities. *Nat Rev*  
504            *Microbiol* 13:388–396.
- 505    20.    Valentine DL, Mezić I, Maćešić S, Črnjarić-Žić N, Ivić S, Hogan PJ,  
506            Fonoberov VA, Loire S. 2012. Dynamic autoinoculation and the microbial  
507            ecology of a deep water hydrocarbon irruption. *Proc Natl Acad Sci U S A*

- 508 109:20286–20291.
- 509 21. Liu J, Zheng Y, Lin H, Wang X, Li M, Liu Y, Yu MM, Zhao M, Pedentchouk  
510 N, Lea-Smith DJ, Todd JD, Magill CR, Zhang WJ, Zhou S, Song D, Zhong H,  
511 Xin Y, Yu MM, Tian J, Zhang XH. 2019. Proliferation of hydrocarbon-  
512 degrading microbes at the bottom of the Mariana Trench. *Microbiome* 7:1–13.
- 513 22. Mason OU, Hazen TC, Borglin S, Chain PSG, Dubinsky EA, Fortney JL, Han  
514 J, Holman HYN, Hultman J, Lamendella R, MacKelprang R, Malfatti S, Tom  
515 LM, Tringe SG, Woyke T, Zhou J, Rubin EM, Jansson JK. 2012. Metagenome,  
516 metatranscriptome and single-cell sequencing reveal microbial response to  
517 Deepwater Horizon oil spill. *ISME J* 6:1715–1727.
- 518 23. Sass AM, Sass H, Coolen MJL, Cypionka H, Overmann J. 2001. Microbial  
519 Communities in the Chemocline of a Hypersaline Deep-Sea Basin (Urania  
520 Basin, Mediterranean Sea). *Appl Environ Microbiol* 67:5392–402.
- 521 24. Voordouw G, Armstrong SM, Reimer MF, Fouts B, Telang AJ, Shen Y,  
522 Gevertz D. 1996. Characterization of 16s rRNA genes from oil field microbial  
523 communities indicates the presence of a variety of sulfate-reducing,  
524 fermentative, and sulfide-oxidizing bacteria. *Appl Environ Microbiol* 62:1623–  
525 1629.
- 526 25. Dubinsky EA, Conrad ME, Chakraborty R, Bill M, Borglin SE, Hollibaugh JT,  
527 Mason OU, M. Piceno Y, Reid FC, Stringfellow WT, Tom LM, Hazen TC,  
528 Andersen GL. 2013. Succession of hydrocarbon-degrading bacteria in the

- 529 aftermath of the deepwater horizon oil spill in the gulf of Mexico. *Environ Sci*  
530 *Technol* 47:10860–10867.
- 531 26. Delmont TO, Hammar KM, Ducklow HW, Yager PL, Post AF. 2014.  
532 *Phaeocystis antarctica* blooms strongly influence bacterial community  
533 structures in the Amundsen Sea polynya. *Front Microbiol* 5:1–13.
- 534 27. Kim S-J, Kim J-G, Lee S-H, Park S-J, Gwak J-H, Jung M-Y, Chung W-H,  
535 Yang E-J, Park J, Jung J, Hahn Y, Cho J-C, Madsen EL, Rodriguez-Valera F,  
536 Hyun J-H, Rhee S-K. 2019. Genomic and metatranscriptomic analyses of  
537 carbon remineralization in an Antarctic polynya. *Microbiome* 7:1–15.
- 538 28. Cordone A, Errico GD, Magliulo M, Bolinesi F, Basili M, Marco R De,  
539 Saggiomo M, Rivaro P. 2021. Bacterioplankton Diversity and Distribution in  
540 Relation to Phytoplankton Community Structure in the Ross Sea surface  
541 waters. *bioRxiv Microbiol*.
- 542 29. Sipler RE, Kellogg CTE, Connelly TL, Roberts QN, Yager PL, Bronk DA.  
543 2017. Microbial community response to terrestrially derived dissolved organic  
544 matter in the coastal Arctic. *Front Microbiol* 8:1018.
- 545 30. Delmont TO, Murat Eren A, Vineis JH, Post AF. 2015. Genome  
546 reconstructions indicate the partitioning of ecological functions inside a  
547 phytoplankton bloom in the Amundsen Sea, Antarctica. *Front Microbiol* 6.
- 548 31. Yang Q, Gao C, Jiang Y, Wang M, Zhou X, Shao H, Gong Z, McMinn A.  
549 2019. Metagenomic characterization of the viral community of the South Scotia

- 550 Ridge. *Viruses* 11:1–19.
- 551 32. Bolger AM, Lohse M, Usadel B. 2014. Trimmomatic: A flexible trimmer for  
552 Illumina sequence data. *Bioinformatics* 30:2114–2120.
- 553 33. Simpson JT, Wong K, Jackman SD, Schein JE, Jones SJM, Birol I. 2009.  
554 ABySS: A parallel assembler for short read sequence data. *Genome Res*  
555 19:1117–1123.
- 556 34. Xu M, Guo L, Gu S, Wang O, Zhang R, Peters BA, Fan G, Liu X, Xu X, Deng  
557 L, Zhang Y. 2020. TGS-GapCloser: A fast and accurate gap closer for large  
558 genomes with low coverage of error-prone long reads. *Gigascience* 9:1–11.
- 559 35. Besemer J, Lomsadze A, Borodovsky M. 2001. GeneMarkS: A self-training  
560 method for prediction of gene starts in microbial genomes. Implications for  
561 finding sequence motifs in regulatory regions. *Nucleic Acids Res* 29:2607–  
562 2618.
- 563 36. Lowe TM, Chan PP. 2016. tRNAscan-SE On-line: integrating search and  
564 context for analysis of transfer RNA genes. *Nucleic Acids Res* 44:W54–W57.
- 565 37. Katoh K, Rozewicki J, Yamada KD. 2018. MAFFT online service: Multiple  
566 sequence alignment, interactive sequence choice and visualization. *Brief*  
567 *Bioinform* 20:1160–1166.
- 568 38. Minh BQ, Schmidt HA, Chernomor O, Schrempf D, Woodhams MD, Von  
569 Haeseler A, Lanfear R, Teeling E. 2020. IQ-TREE 2: New Models and  
570 Efficient Methods for Phylogenetic Inference in the Genomic Era. *Mol Biol*



- 571 Evol 37:1530–1534.
- 572 39. Letunic I, Bork P. 2019. Interactive Tree of Life (iTOL) v4: Recent updates  
573 and new developments. *Nucleic Acids Res* 47:256–259.
- 574 40. Roux S, Páez-Espino D, Chen IMA, Palaniappan K, Ratner A, Chu K, Reddy  
575 T, Nayfach S, Schulz F, Call L, Neches RY, Woyke T, Ivanova NN, Eloe-  
576 Fadrosh EA, Kyrpides NC. 2021. IMG/VR v3: An integrated ecological and  
577 evolutionary framework for interrogating genomes of uncultivated viruses.  
578 *Nucleic Acids Res* 49:D764–D775.
- 579 41. Moraru C, Varsani A, Kropinski AM. 2020. VIRIDIC — A Novel Tool to  
580 Calculate the Intergenomic Similarities of. *Viruses* 12:1268.
- 581 42. Lee I, Kim YO, Park SC, Chun J. 2016. OrthoANI: An improved algorithm and  
582 software for calculating average nucleotide identity. *Int J Syst Evol Microbiol*  
583 66:1100–1103.
- 584 43. Nishimura Y, Yoshida T, Kuronishi M, Uehara H, Ogata H, Goto S. 2017.  
585 ViPTree: The viral proteomic tree server. *Bioinformatics* 33:2379–2380.
- 586 44. Hall TMT, Porter JA, Beachy PA, Leahy DJ. 1995. A potential catalytic site  
587 revealed by the 1.7-Å crystal structure of the amino-terminal signalling domain  
588 of Sonic hedgehog. *Nat* 1995 378:212–216.
- 589 45. Owens AE, Iannuzzelli JA, Gu Y, Fasan R. 2020. MOrPH-PhD: An Integrated  
590 Phage Display Platform for the Discovery of Functional Genetically Encoded  
591 Peptide Macrocycles. *ACS Cent Sci* 6:368–381.

- 592 46. Dawber RJ, Hebbes S, Herpers B, Docquier F, Van Den Heuvel M. 2005.  
593 Differential range and activity of various forms of the Hedgehog protein. *BMC*  
594 *Dev Biol* 5:1–14.
- 595 47. Khakhum N, Yordpratum U, Boonmee A, Tattawasart U, Rodrigues JLM,  
596 Sermswan RW. 2016. Cloning, expression, and characterization of a  
597 peptidoglycan hydrolase from the *Burkholderia pseudomallei* phage ST79.  
598 *AMB Express* 6.
- 599 48. Roelink H. 2018. Sonic Hedgehog is a member of the Hh/DD-peptidase family  
600 that spans the eukaryotic and bacterial domains of life. *J Dev Biol* 6:1–11.
- 601 49. Decewicz P, Radlinska M, Dziewit L. 2017. Characterization of *Sinorhizobium*  
602 sp. LM21 prophages and virus-encoded DNA methyltransferases in the light of  
603 comparative genomic analyses of the sinorhizobial virome. *Viruses* 9:1–19.
- 604 50. Dna FOF. 1995. Function of Dna. *New York* 293–318.
- 605 51. Liu J, Mushegian A. 2004. Displacements of prohead protease genes in the late  
606 operons of double-stranded-DNA bacteriophages. *J Bacteriol* 186:4369–4375.
- 607 52. Zheng D, Xu Y, Yuan G, Wu X, Li Q. 2021. Bacterial ClpP Protease Is a  
608 Potential Target for Methyl Gallate. *Front Microbiol* 11:1–10.
- 609 53. Kauffman KM, Hussain FA, Yang J, Arevalo P, Brown JM, Chang WK,  
610 Vaninsberghe D, Elsherbini J, Sharma RS, Cutler MB, Kelly L, Polz MF. 2018.  
611 A major lineage of non-tailed dsDNA viruses as unrecognized killers of marine  
612 bacteria. *Nature* 554:118–122.

- 613 54. Ramos JL, Martínez-Bueno M, Molina-Henares AJ, Terán W, Watanabe K,  
614 Zhang X, Gallegos MT, Brennan R, Tobes R. 2005. The TetR Family of  
615 Transcriptional Repressors. *Microbiol Mol Biol Rev* 69:326–356.
- 616 55. Colclough AL, Scadden J, Blair JMA. 2019. TetR-family transcription factors  
617 in Gram-negative bacteria: Conservation, variation and implications for efflux-  
618 mediated antimicrobial resistance. *BMC Genomics* 20:1–12.
- 619 56. Uchiyama J, Rashel M, Takemura I, Wakiguchi H, Matsuzaki S. 2008. In silico  
620 and in vivo evaluation of bacteriophage  $\phi$ EF24C, a candidate for treatment of  
621 *Enterococcus faecalis* infections. *Appl Environ Microbiol* 74:4149–4163.
- 622 57. Bin Jang H, Bolduc B, Zablocki O, Kuhn JH, Roux S, Adriaenssens EM,  
623 Brister JR, Kropinski AM, Krupovic M, Lavigne R, Turner D, Sullivan MB.  
624 2019. Taxonomic assignment of uncultivated prokaryotic virus genomes is  
625 enabled by gene-sharing networks. *Nat Biotechnol*.
- 626 58. Kang I, Oh HM, Kang D, Cho JC. 2013. Genome of a SAR116 bacteriophage  
627 shows the prevalence of this phage type in the oceans. *Proc Natl Acad Sci U S*  
628 *A* 110:12343–12348.
- 629 59. Zhao Y, Temperton B, Thrash JC, Schwalbach MS, Vergin KL, Landry ZC,  
630 Ellisman M, Deerinck T, Sullivan MB, Giovannoni SJ. 2013. Abundant SAR11  
631 viruses in the ocean. *Nature* 494:357–360.
- 632 60. Hurwitz BL, Sullivan MB. 2013. The Pacific Ocean Virome (POV): A Marine  
633 Viral Metagenomic Dataset and Associated Protein Clusters for Quantitative

- 634 Viral Ecology. PLoS One 8.
- 635 61. Yan Liu, Pavla Debeljak, Mathieu Rembauville, Stéphane Blain IO. 2019.
- 636 Diatoms shape the biogeography of heterotrophic prokaryotes in early spring in
- 637 the Southern Ocean. Environ Microbiol 21:1452–1465.
- 638 62. Kim J-G, Park S-J, Quan Z-X, Jung M-Y, Cha I-T, Kim S-J, Kim K-H, Yang
- 639 E-J, Kim Y-N, Lee S-H, Rhee S-K. 2013. Unveiling abundance and
- 640 distribution of planktonic Bacteria and Archaea in a polynya in Amundsen Sea,
- 641 Antarctica <https://doi.org/10.1111/1462-2920.12287>.
- 642 63. Ghiglione J-F, Galand PE, Pommier T, Pedrós-Alió C, Maas EW, Bakker K,
- 643 Bertilson S, Kirchman DL, Lovejoy C, Yager PL, Murray AE, Karl DM. Pole-
- 644 to-pole biogeography of surface and deep marine bacterial communities
- 645 <https://doi.org/10.1073/pnas.1208160109>.
- 646 64. Delong EF, Baumann L, Bowditch RD, Baumann P. 1984. Microbiology 9
- 647 170–178.
- 648 65. Henson SA, Cael BB, Allen SR, Dutkiewicz S. 2021. Future phytoplankton
- 649 diversity in a changing climate. Nat Commun 12:1–8.
- 650 66. Gray A, Krolikowski M, Fretwell P, Convey P, Peck LS, Mendelova M, Smith
- 651 AG, Davey MP. 2020. Remote sensing reveals Antarctic green snow algae as
- 652 important terrestrial carbon sink. Nat Commun 11.
- 653 67. Lutz S, Anesio AM, Raiswell R, Edwards A, Newton RJ, Gill F, Benning LG.
- 654 2016. The biogeography of red snow microbiomes and their role in melting

- 655 arctic glaciers. *Nat Commun* 7:1–9.
- 656 68. Croft MT, Lawrence AD, Raux-Deery E, Warren MJ, Smith AG. 2005. Algae  
657 acquire vitamin B12 through a symbiotic relationship with bacteria. *Nature*  
658 438:90–93.
- 659 69. Bertrand EM, McCrow JP, Moustafa A, Zheng H, McQuaid JB, Delmont TO,  
660 Post AF, Sipler RE, Spackeen JL, Xu K, Bronk DA, Hutchins DA, Allen AE,  
661 Karl DM. 2015. Phytoplankton-bacterial interactions mediate micronutrient  
662 colimitation at the coastal Antarctic sea ice edge. *Proc Natl Acad Sci U S A*  
663 112:9938–9943.
- 664 70. Oliver H, St-Laurent P, Sherrell RM, Yager PL. 2019. Modeling Iron and Light  
665 Controls on the Summer *Phaeocystis antarctica* Bloom in the Amundsen Sea  
666 Polynya. *Global Biogeochem Cycles* <https://doi.org/10.1029/2018GB006168>.
- 667 71. Mönnich J, Tebben J, Bergemann J, Case R, Wohlrab S, Harder T. 2020.  
668 Niche-based assembly of bacterial consortia on the diatom *Thalassiosira rotula*  
669 is stable and reproducible. *ISME J* 14:1614–1625.
- 670 72. Luria CM, Amaral-Zettler LA, Ducklow HW, Rich JJ. 2016. Seasonal  
671 succession of free-living bacterial communities in coastal waters of the western  
672 antarctic peninsula. *Front Microbiol* 7:1–13.
- 673
- 674

**Table 1 Amino acid identity of Oceanospirillum phage vB\_OsaM\_PD0307 and other night homologous sequences.**

Abbreviation	Identity Frequency		Bit-score Frequency	
	mean	median	mean	median
IMGVR_UViG_3300009431_000281	85.08	93.7	428.9	346.5
S137_MES_NO_1159	83.36	87.01	461.6	343
S85_DCM_NO_526	72.9	79.04	428.2	282
Shewanella phage SppYZU01	48.33	47.22	260.6	173
S201_DCM_NO_1678	48.24	47.73	260.4	144
IMGVR_UViG_3300003691_000130	46.53	46.51	247.9	125
S82_SUR_NO_687	45.45	44.27	249.1	159
IMGVR_UViG_3300024520_000016	40.97	37.32	127.7	30

676 **Figure legends**

677 **Fig. 1** (A) Morphology and biological properties of phage vB\_OsaM\_PD0307, the scale  
678 bar is 50 nm. (B) Phage plaques of vB\_OsaM\_PD0307 formed in double-layer agar  
679 plates, the scale bar is 5 mm

680 **Fig. 2** The maximum likelihood phylogenetic tree of *Oceanospirillum* sp. PD0307 and  
681 16S rRNA sequences of 31 related *Oceanospirillaceae* species. The *Oceanospirillum*  
682 sp. PD0307 was highlighted in the tree. A relatively close relationship of  
683 *Oceanospirillum* sp. PD0307 with other *Oceanospirillum* was displayed, while  
684 monophyly of its branch was observed.

685

686 **Fig. 3** Circularized genome map (A) and cumulative GC skew analysis (B) of the  
687 genome sequence of *Oceanospirillum* phage vB\_OsaM\_PD0307. (A) The outer circle  
688 represents different categories of putative functional genes, which were represented by  
689 different colors. (B) the cumulative graph of minimum and maximum values of GC  
690 skew were displayed and calculated by using a window size of 1,00 bp and a step size  
691 of 100 bp. The GC-skew and the cumulative GC-skew were represented by blue and  
692 red lines, respectively. The minimum and maximum of a GC-skew could be used to  
693 predict the origin of replication (300 nt) and the terminus location (43900 nt).

694

695 **Fig. 4** Phylogenetic trees of *Oceanospirillum* Phage vB\_OsaM\_PD0307 with different  
696 references. (A) The whole-genomes phylogenetic tree was constructed with 1,812

697 dsDNA phages genomes in the Virus-Host database as references. (B) Nine  
698 *Oceanospimyovirus* (Oceanospirillum Phage vB\_OsaM\_PD0307, Shewanella phage  
699 SppYZU01, and seven homologous uncultured viral genomes) as queries and other 80  
700 related phages were used to construct a circular phylogenetic tree. (C) A rectangular  
701 phylogenetic tree was established with *Oceanospimyovirus* and seven Mycobacterium  
702 phages, which were used as outgroups for control. (D) Gene synteny of  
703 Oceanospirillum Phage vB\_OsaM\_PD0307, Shewanella phage SppYZU01, and seven  
704 homologous uncultured viral genomes in IMG/VR v3 database. Sequences comparison  
705 performed using tBLASTx (10 bp minimum alignment) with percent identity. Synteny  
706 was recognized when genomes featured a minimum of five consecutive syntenic genes  
707 within the same genomic area and separated by a maximum of four non-syntenic genes.  
708

709 **Fig. 5** (A) Heatmap of intergenomic similarity values (right half) and alignment  
710 indicators (left half and top annotation) of eight *Oceanospirillaceae* phages and eight  
711 homologous uncultured viral genomes of Oceanospirillum Phage vB\_OsaM\_PD0307.  
712 The numbers of intergenomic similarity values represent the similarity values for each  
713 genome pair, rounded to the first decimal. The genome length ratio for a genome pair  
714 using a black to white color gradient indicator. The aligned fraction genome was  
715 indicated by orange to white color gradient. (B) The average nucleotide sequence  
716 identity (ANI) of Oceanospirillum Phage vB\_OsaM\_PD0307, Shewanella phage  
717 SppYZU01, and seven homologous uncultured viral contigs based on OrthoANI values



718 calculated using OAT software.

719

720 **Fig. 6** Relative abundance of Oceanospirillum Phage vB\_OsaM\_PD0307, Shewanella

721 phage SppYZU01, seven homologous uncultured viral contigs and reference phage

722 genomes in the global ocean viromes (GOV 2.0) datasets.

723

724 **SUPPLEMENTAL MATERIAL**

725 Supplemental material is available online only.

726 FIG S1, PDF file, 6321 KB.

727 TABLE S1, XLSX file, 17 KB.

728 TABLE S2, XLSX file, 14 KB.

729 TABLE S3, XLSX file, 28 KB.

730 **Supplemental file 1: Fig S1** Amino acid identity and bitscore distribution between

731 vB\_OsaM\_PD0307, Shewanella phage SppYZU01, and seven homologous uncultured

732 viral genomes

733 **Supplemental file 2: Table S1** Genome annotation of Oceanospirillum phage

734 vB\_OsaM\_PD0307

735 **Supplemental file 3: Table S2** The result of BLASTn in IMG/VR and the uncultured

736 contigs' information

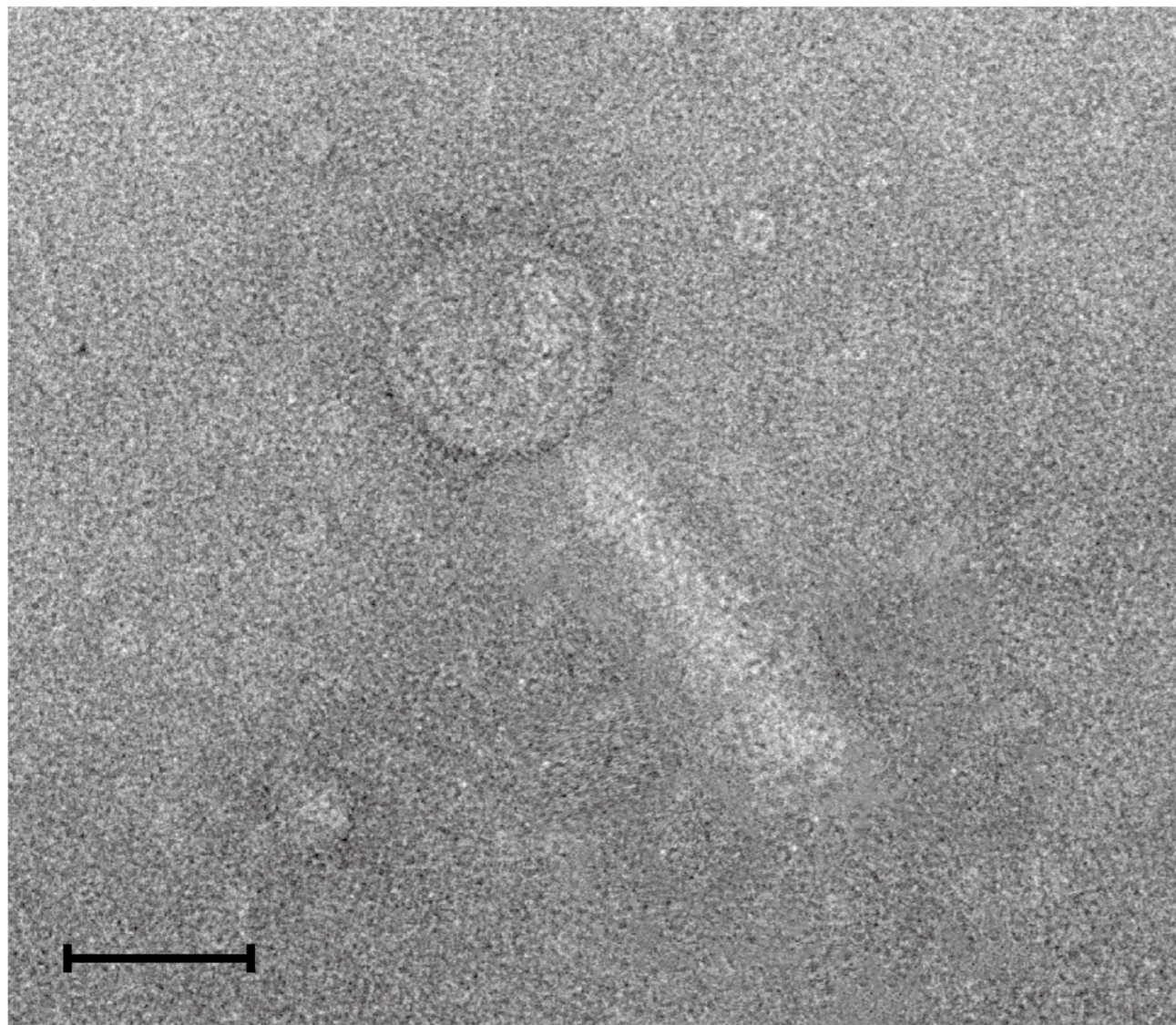
737 **Supplemental file 4: Table S3** Average amino acid identity of Oceanospirillum Phage

738 vB\_OsaM\_PD0307 between Shewanella phage SppYZU01 and seven homologous

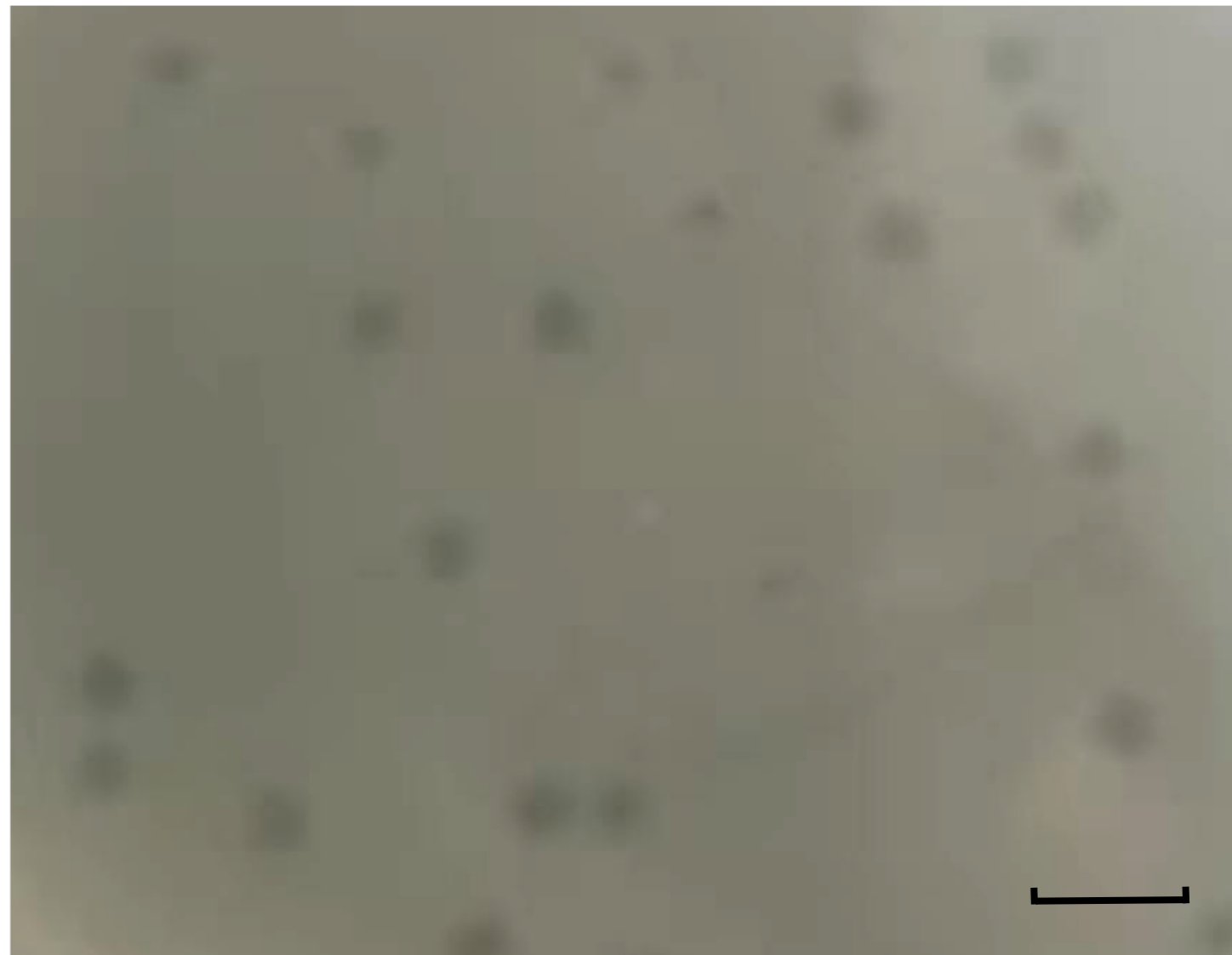
739 uncultured viral genomes

740

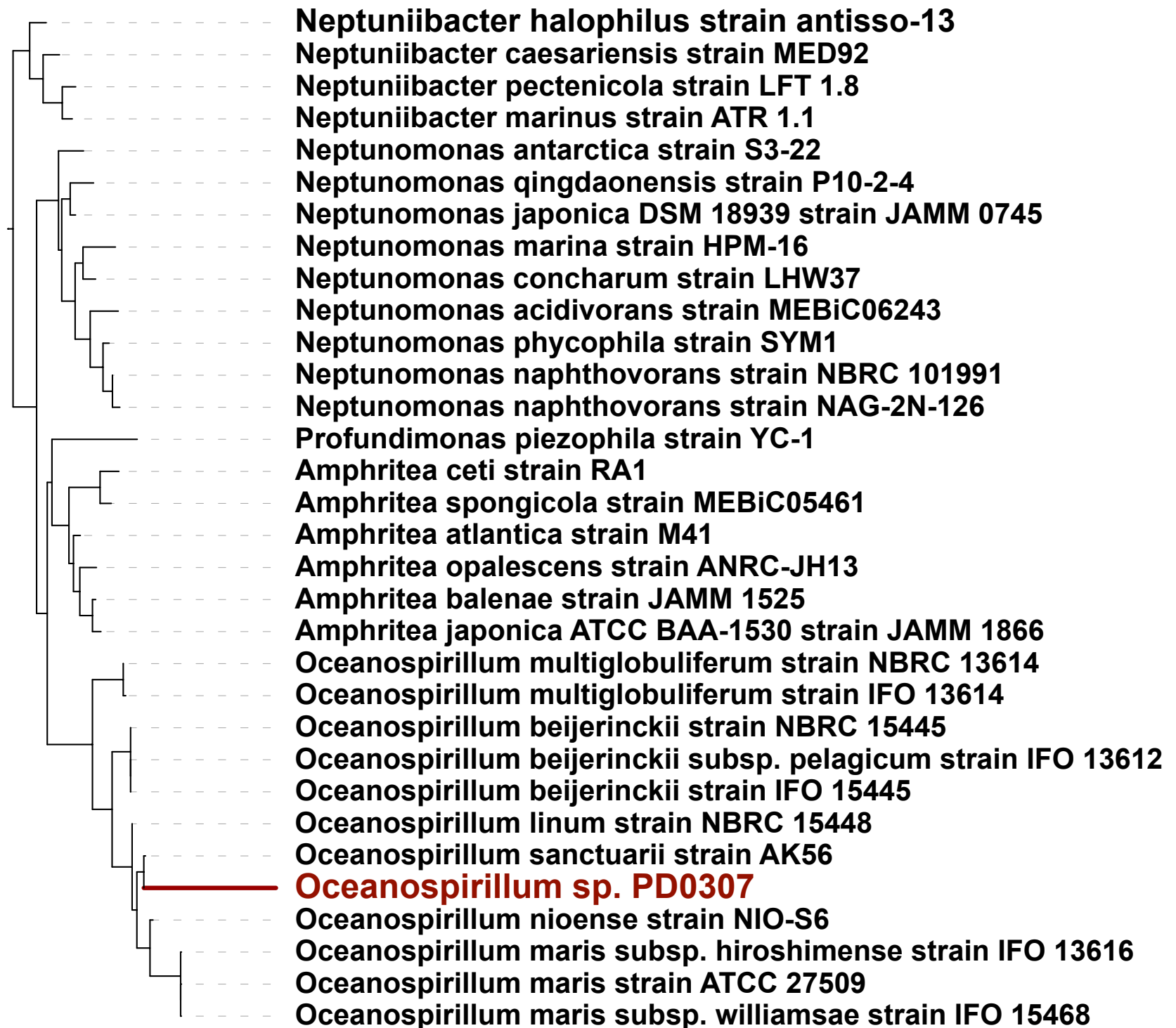
**A**

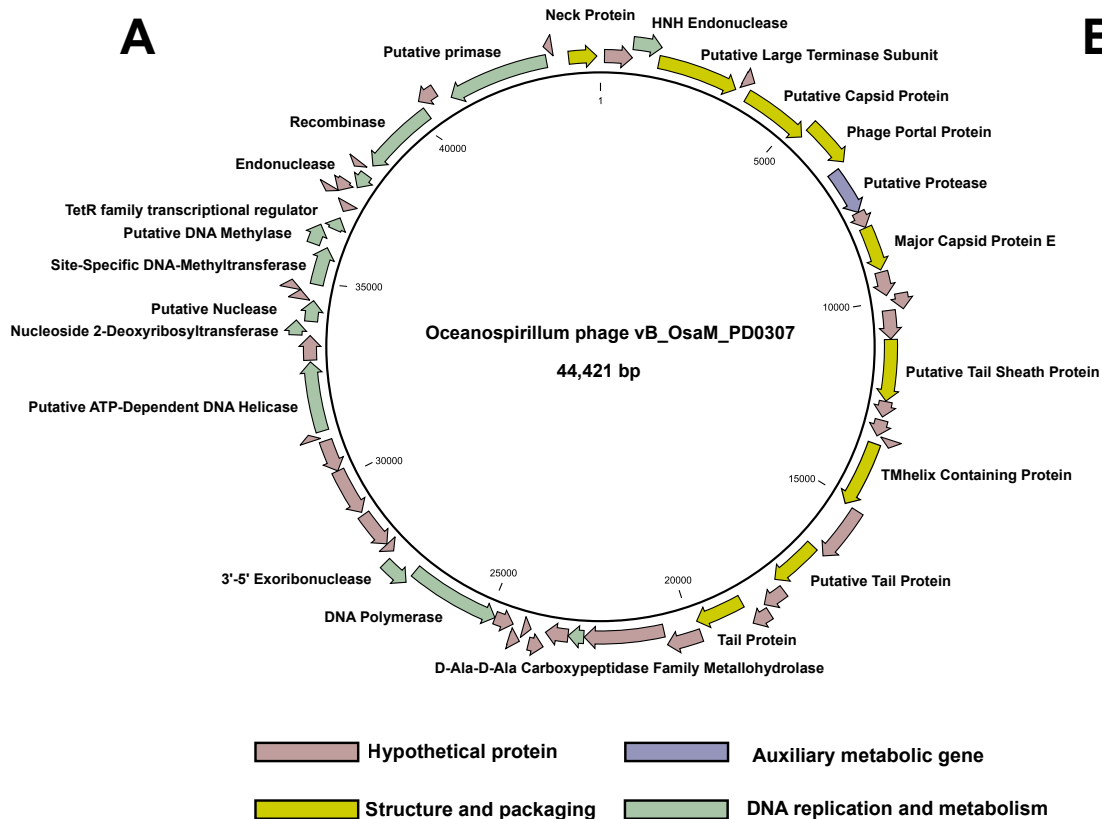
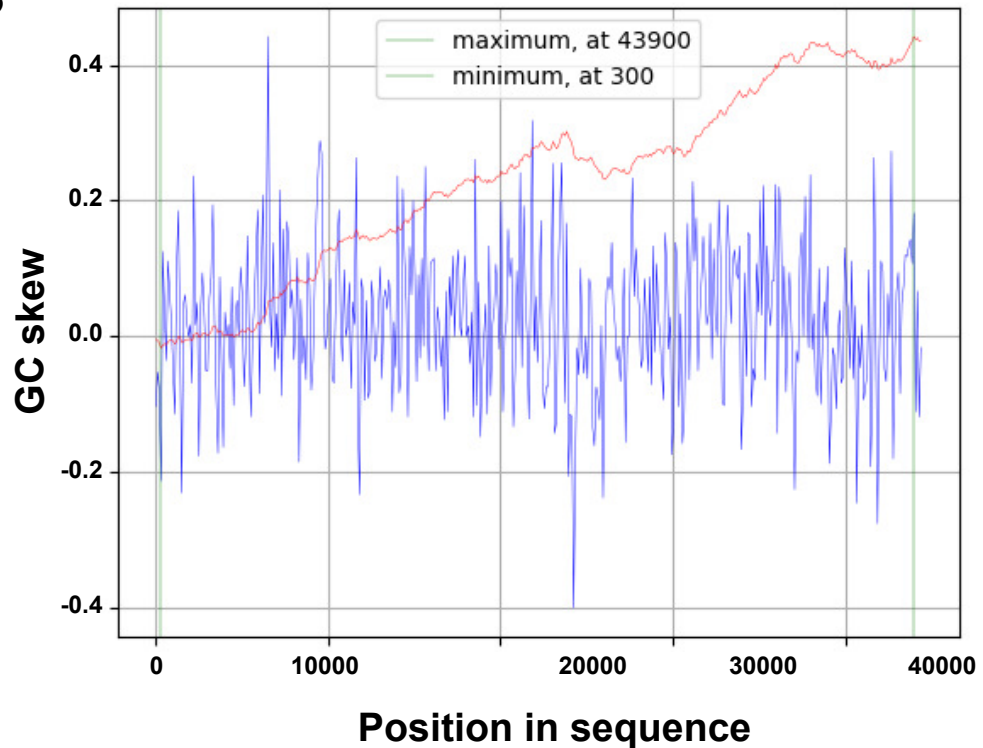


**B**

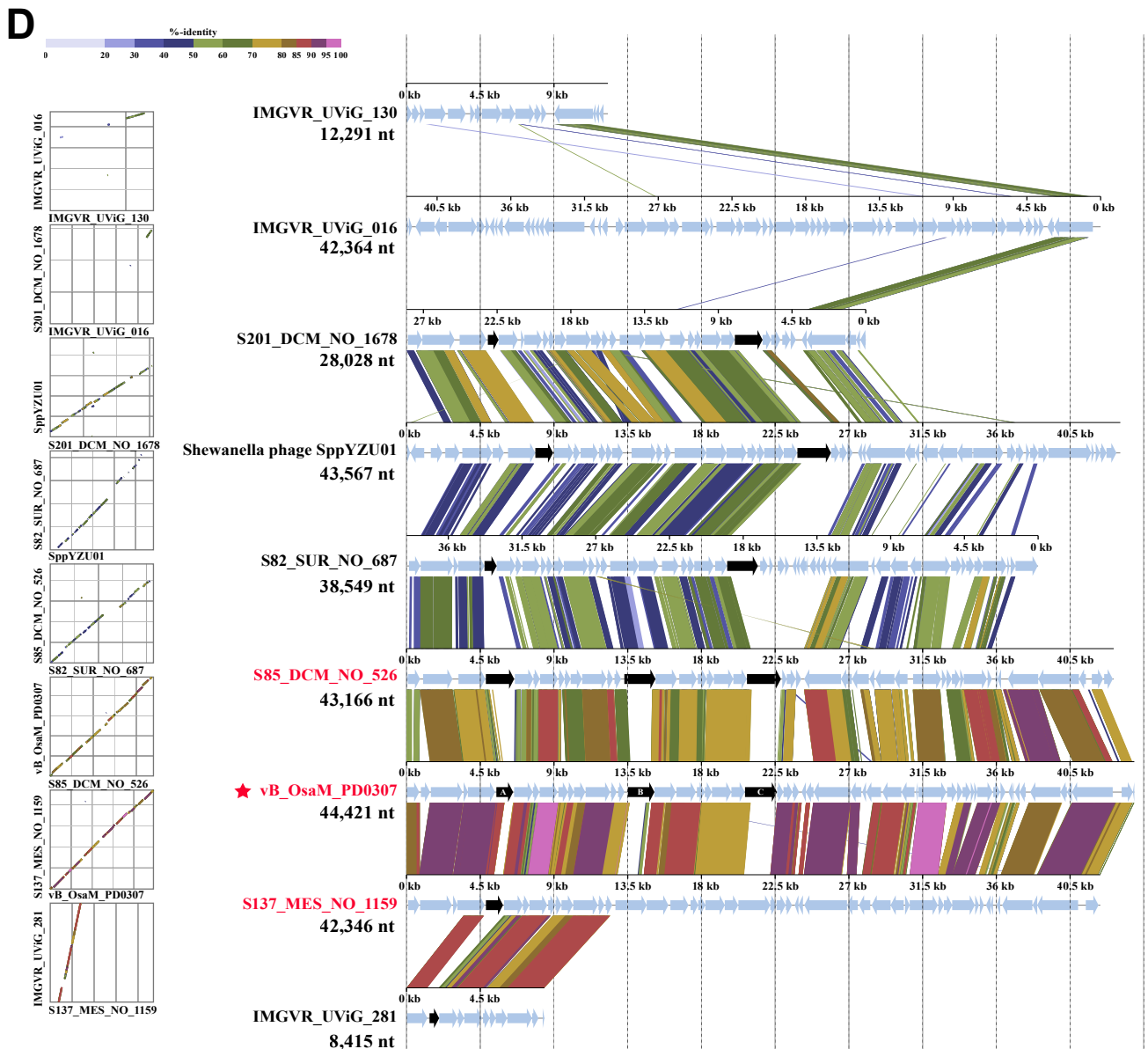
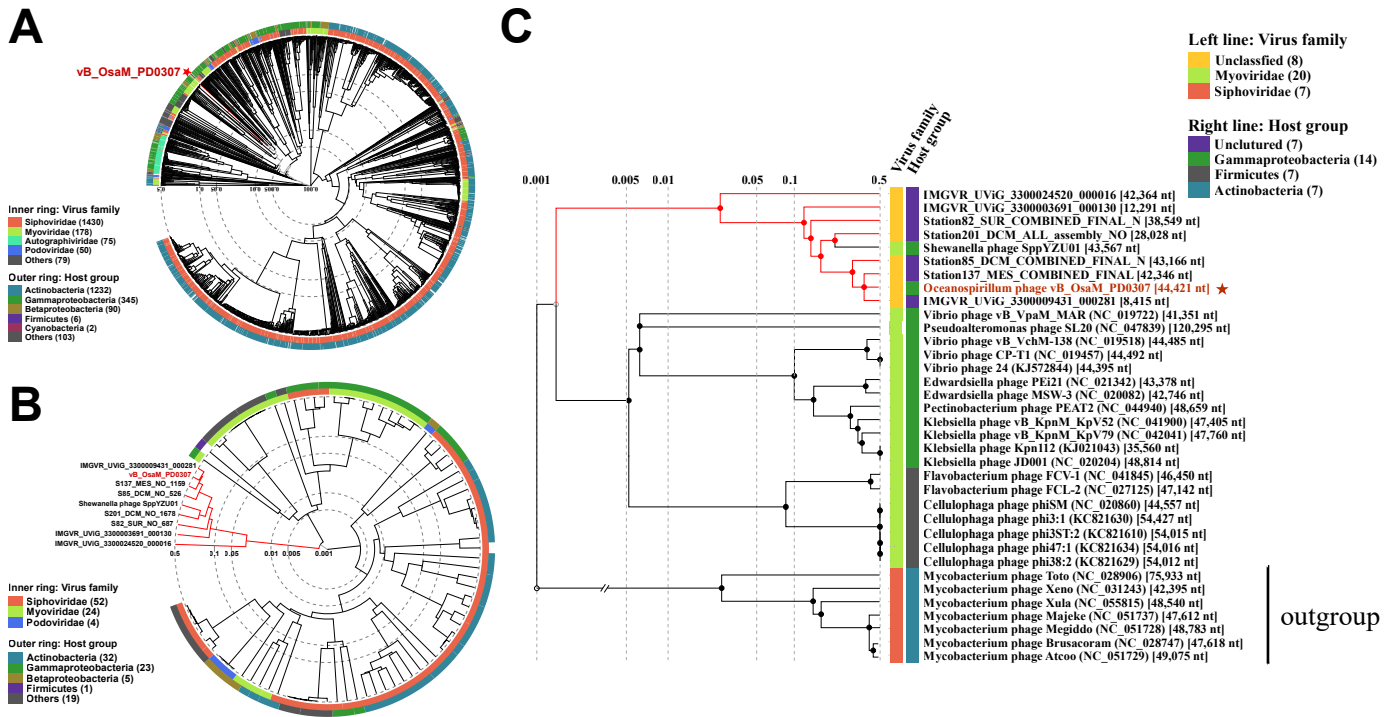


Tree scale: 0.03



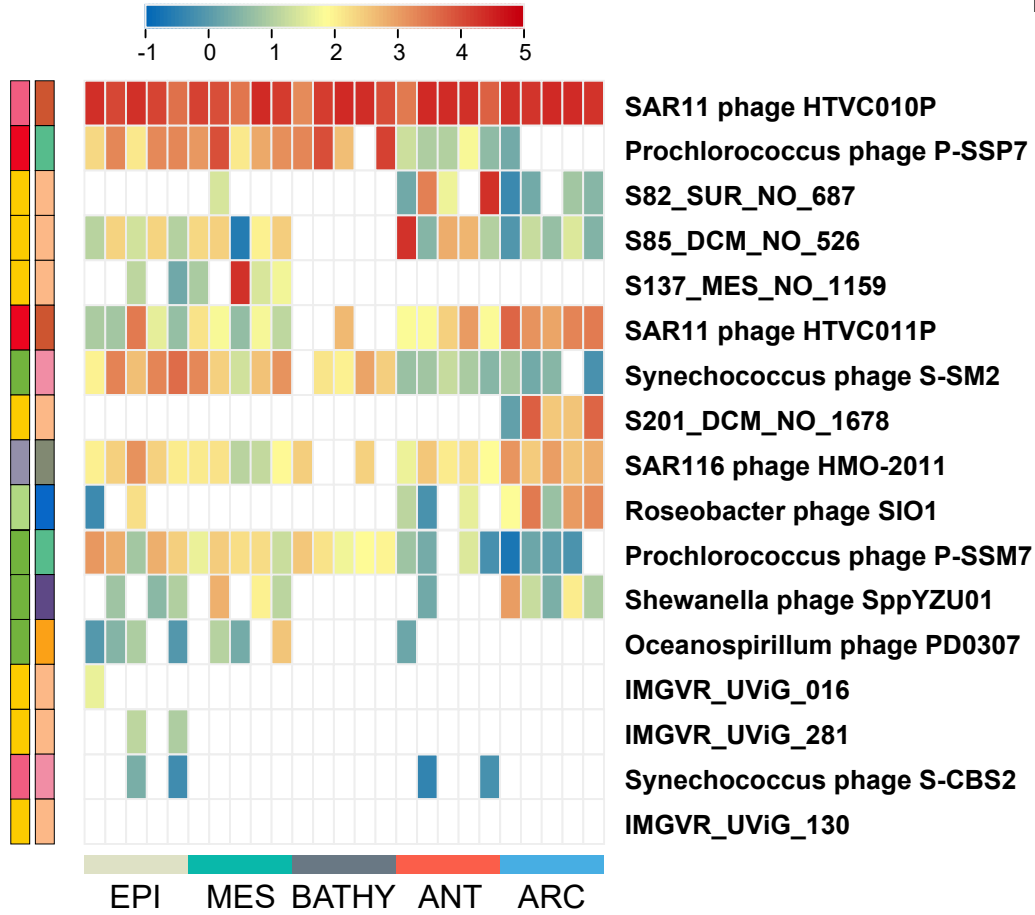
**A****B**



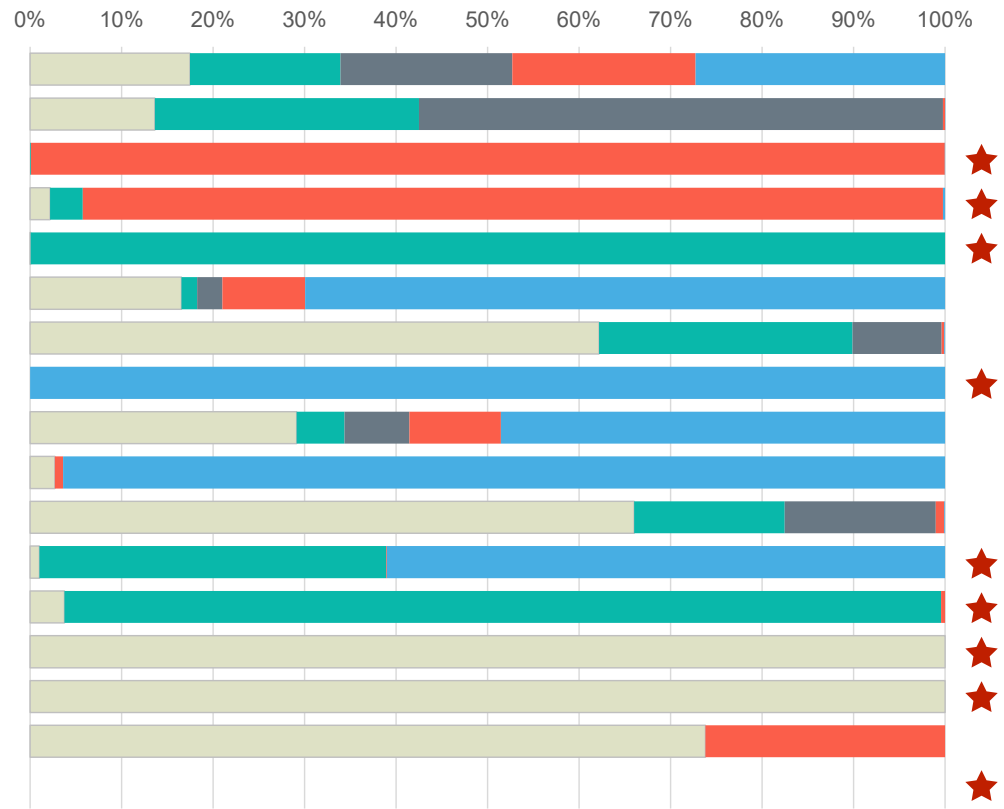




### Relative abundance of viruses (Log10 RPKM)



### Percentage of the relative abundance of viruses in each marine VEZ



#### Left line: Virus family

- *Myoviridae* (4)
- *Autographiviridae* (2)
- *Podoviridae* (1)
- *Zobellviridae* (1)
- *Siphoviridae* (2)
- unclassified (7)

#### Right line: Host group

- *Oceanospirillaceae* (1)
- *Pelagibacteraceae* (2)
- *Shewanellaceae* (1)
- *Prochlorococcaceae* (2)
- uncltured (7)
- *Synechococcaceae* (2)
- *SAR116 cluster* (1)
- *Roseobacteraceae* (1)

#### Viral ecological zones

- EPI
- MES
- BATHY
- ANT
- ARC



**Table 1 Amino acid identity of Oceanospirillum phage vB\_OsaM\_PD0307 and other night homologous sequences.**

Abbreviation	Identity		Bit-score	
	Frequency		Frequency	
	mean	median	mean	median
IMGVR_UViG_281	85.08	93.7	428.9	346.5
S137_MES_NO_1159	83.36	87.01	461.6	343
S85_DCM_NO_526	72.9	79.04	428.2	282
Shewanella phage SppYZU01	48.33	47.22	260.6	173
S201_DCM_NO_1678	48.24	47.73	260.4	144
IMGVR_UViG_130	46.53	46.51	247.9	125
S82_SUR_NO_687	45.45	44.27	249.1	159
IMGVR_UViG_016	40.97	37.32	127.7	30